Biogeosciences Discuss., doi:10.5194/bg-2017-151, 2017
Manuscript under review for journal Biogeosciences
Discussion started: 17 May 2017


# Historic carbon burial spike in an Amazon floodplain lake linked to riparian deforestation near Santarem, Brazil

Luciana M. Sanders[1], Kathryn Taffs[1], Debra Stokes[3], Christian J. Sanders[2], Alex Enrich-Prast[4,5], Leonardo Nogueira Amora[6,7], Humberto Marotta[6,7]

*[1]Southern Cross Geoscience, Southern Cross University, P.O. Box 157, Lismore, NSW 2480, Australia.*
*[2]National Marine Science Centre, School of Environment, Science and Engineering, Southern Cross University, Coffs Harbour, New South Wales, Australia.*
*[3]Marine Ecology Research Centre, Southern Cross University, P.O. Box 157, Lismore, NSW 2480, Australia University, P.O. Box 157, Lismore, NSW 2480, Australia.*
*[4]Laboratório de Biogeoquímica, Universidade Federal do Rio de Janeiro (UFRJ), Rio d Janeiro (RJ), 21941 971, Brazil.*
*[5]Department of Environmental Change, Linköping University, 581 83, Linköping, Sweden.*
*[6]Ecosystems and Global Change Laboratory (LEMG-UFF) / International Laboratory of Global Change (LINCGlobal). Biomass and Water Management Research Center (NAB-UFF). Graduated Program in Geosciences (Environmental Geochemistry). Universidade Federal Fluminense (UFF), Av. Edmundo March, s/nº – Zip Code: 24210-310, Niteroi/RJ- Brazil.*
*[7]Sedimentary and Environmental Processes Laboratory (LAPSA-UFF). Department of Geography. Graduated Program in Geography. Universidade Federal Fluminense (UFF), Av. Gal. Milton Tavares de Souza, s/nº - Zip Code: 24210-346, Niteroi/RJ- Brazil.*

*Corresponding author. E-mail address; l.sanders.13@student.scu.edu.au

**Abstract**

The forests along the Amazon Basin produce significant quantities of organic material, a portion of which is deposited in floodplain lakes. However, potentially important effects of ongoing deforestation in the watershed on these carbon fluxes is still poorly understood. Here, a sediment core was extracted from an Amazon floodplain lake to examine the relationship between carbon burial and land cover/use. Historical records from 1942 and satellite data from 1975 were used to calculate deforestation rates between 1942 and 1975, and 1975 to 2008 in four zones with different distances from the margins of the lake and its tributaries (100, 500, 1000 and 6000-m buffers). Sediment accumulation rates were determined from the $^{240+239}Pu$ signatures and the excess $^{210}Pb$ method, reaching near 3.8 and 4.2 mm year$^{-1}$ in the last 60 and 120 years respectively. The average carbon burial rates ranged between 100 and 350 g C m$^{-2}$ year$^{-1}$, with pulses of high carbon burial derived from the forest vegetation, as indicated by $\delta^{13}C$ and $\delta^{15}N$ signatures, which corresponded to heavy deforestation in the 1940 and 50s. Finally, our results revealed a potentially important spatial dependence of the OC burial in Amazon lacustrine sediments in relation to deforestation rates in the catchment. These deforestation rates were more intense in the riparian vegetation (100-m buffer) during the period 1942-1975 and the larger open water areas (500, 1000 and 6000-m buffer) during 1975-2008. The continued removal of vegetation from the interior of the forest was not related to the peak of OC burial in the lake, but only the riparian deforestation around 1950. Our novel findings suggest the importance of abrupt and temporary events in which some of the biomass released by the deforestation, especially restricted to areas along open water edges, might reach the depositional environments in the floodplain of the Amazon Basin.

Biogeosciences Discuss., doi:10.5194/bg-2017-151, 2017
Manuscript under review for journal Biogeosciences
Discussion started: 17 May 2017


## 1. Introduction

Rivers act as vectors, transporting sediment from land to ocean (Abril et al. 2014). Along this trajectory a significant proportion of the sediment load, including organic material, may be deposited in floodplains, creating zones of carbon accumulation (Smith et al. 2002, Dong et al. 2012, Hoffmann et al. 2013). This process is accelerated during flood events, when rivers and tributaries deposit organic material along the inundated floodplains (Smith et al. 2002). In some climate zones floodplains are seasonally inundated, with riparian zone vegetation dependent upon this seasonal influx of organic material. The vegetation acts to slow water velocity and trap the fine-grained, carbon rich sediment, within the low-energy environment (Aalto et al. 2003). Therefore, the riparian vegetation along her floodplains may be important for the organic matter deposition and the Amazon carbon cycle.

The importance of tropical wetland ecosystems in the carbon cycle is well documented (Downing et al. 1993, Melack et al. 2004, Zocatelli et al. 2013, Abril et al. 2014, Marotta et al. 2014). It has been shown that wetlands in the warm tropics are some of the most productive biological communities in the world (Neue et al. 1997), representing an important sink for nutrients (Marotta et al. 2009) and carbon (Peixoto et al. 2016), as well as sources of organic substrates to carbon gas production in inland waters (Marotta et al. 2010). However, these wetland ecosystems are also highly threatened by land use activities, especially from deforestation, development of agricultural land and soil degradation (Junk 2013, Lucas et al. 2014). For example, the Amazon Basin wetlands are being degraded by farming activities such as commercial ranching, and an increase in road density (Goulding 1993).

Deforestation of the Amazon Basin accelerated toward the end of the 1970's (Skole and Tucker 1993), when an estimated 15% of the pristine rainforest area was lost by the year 2003, increasing to approximately 18% by 2015 (INPE 2016). The ongoing loss of vegetation is responsible for a substantial increase in erosion rates and subsequent sediment inputs into Amazon rivers and lakes (Neill et al. 2013b). Yet these anthropogenic activities are potential sources of allochthonous organic matter that may increase carbon stores in the associated floodplain areas (Diaz and Rosenberg 2008, Stanley et al. 2012).

The city of Santarem, in central Amazon, was established in the mid-eighteenth century, approximately 650 km upstream from the Amazon River mouth and at its confluence with the River Tapajós (02°25'0.28"S and 54°42'41.57"W, Figure 1). In 1940, Santarém was only a small village with less than 0.5 km$^2$, surrounded by dense pristine rainforest (estimation from the historical mapping of the Santarém City Hall). This city quickly expanded, occupying 5.2 km$^2$ by the end of the 1970s and 49.3 km$^2$ currently (estimation from satellite images LANDSAT/SRTM). Jupindá Lake is 70 km East of from Santarém City, and receives surface water inflow from small streams draining from the forest and the main tributary Curuá-Una River, a large affluent of the Amazon River (Figure 1). The Lake has been affected by the deforestation associated with the expansion of Santarém City. Between the 1940's and 1950's, there was intense deforestation on the margins of rivers and streams in this area, used to supply the market of wood and forestry products (Amorim 2000, Cruz et al. 2011). In the 1970s, the Curuá-Una River was dammed (Curuá-Una Dam) 45 km upstream of Jupindá Lake to build the first hydroelectric plant of the Amazon Forest (LigockI 2003).

Jupindá Lake provides an ideal opportunity to investigate historical changes in organic carbon burial in a floodplain lake as a result of anthropogenic activities. This will aid identification of still-little known impacts of land cover changes on recent carbon burial rates in depositional environments of the Amazon floodplain.

The objectives of this research are to investigate the affect deforestation and urban development has on carbon burial rates in a tropical floodplain wetland.

## 2. Methods

A 60 cm depth sediment core (diameter 7.5 cm) was collected in 2010 using a gravity corer in the center of the Jupindá Lake (02°27'43.60" S, 54° 5'1.30" W. The sediment core was sub sampled at 2 cm intervals. Dry bulk density (DBD, g $cm^{-3}$) was determined as the dry sediment weight (g) divided by the initial volume ($cm^3$). A homogenized portion was acidified to remove carbonate material, then dried and ground to powder for organic carbon (OC), nitrogen (N), $\delta^{13}C$, and $\delta^{15}N$ analyses using a Flash Elemental Analyzer coupled to a Thermo Fisher Delta V IRMS (isotope ratio mass spectrometer). Analytical precision: C = 0.1 %, N = 0.1%, $\delta^{13}C$ = 0.1‰ and $\delta^{15}N$ = 0.15 ‰.

Samples were prepared for Pu dating following the method of Ketterer et al. (2004) with modifications to enable larger sample mass to be processed as a result of the likely lower Pu concentrations in the Southern Hemisphere (Sanders et al. 2014). To obtain a larger mass, sediment intervals were joined and homogenized so the sediment intervals for the $^{240+239}Pu$ dating was 4 cm intervals. Sample aliquots ranging from 14 to

29 grams were dry-ashed at 600 $^{O}$C for 16 hours, and leached with 50 mL of 16 M $HNO_3$. The leaching was conducted overnight at 80$^{O}$C with added $^{242}$Pu yield tracer (NIST 4334g, 19 picograms). Acid leaching (as opposed to complete dissolution with HF) is known to solubilize stratospheric fallout Pu, and there is little possibility that “refractory” $HNO_3$-insoluble Pu exists in the South America (Sanders et al. 2014). The leachates were diluted to 100 mL, filtered to remove solids, and the aqueous solutions were processed with TEVA resin (EIChrom, Lisle, Il, USA) in order to chemically isolate 3.0 mL Pu fractions in aqueous ammonium oxalate solution suitable for measurements by sector ICPMS. Pu determinations were performed using a VG Axiom MC operating in the single collector (electron multiplier) mode. The system was used with an APEX HF desolvating micronebulizer system (ESI Scientific, Omaha, NE, USA) with an uptake rate of 0.4 mL/minute. Qualitative mass spectral scans (averages of 50 sweeps over the mass range 237.4 – 242.6) were collected for selected samples prior to the electrostatic sector quantitative scanning of $^{238}$U+, $^{239}$Pu+, $^{240}$Pu+, and $^{242}$Pu+. Detection limits were evaluated based upon the analysis of two blanks and considerations regarding the obtained mass spectra. A detection limit of 0.01 Bq/kg of $^{239+240}$Pu is applicable for samples of nominal 25 g mass.

For $^{210}$Pb dating, an intrinsic germanium detector coupled to a multi-channel analyzer was used. Freeze dried and ground sediments were packed and sealed in gamma tubes. Lead-210 and $^{226}$Ra activities were calculated by multiplying the counts per minute by a factor that includes the gamma-ray intensity and detector efficiency determined from standard calibrations. Identical geometry was used for all samples. Lead-210 activities were determined by the direct measurement of the 46.5 KeV gamma peak. Radium-226 activity was determined via the $^{214}Pb$ daughter at 351.9 KeV. For $^{226}Ra$ measurements, the packed samples were set aside for at least 21 days to allow for $^{222}Rn$ to ingrow and establish secular equilibrium between $^{226}Ra$ and its granddaughter $^{214}Pb$. Excess $^{210}Pb$ activity was calculated by subtracting the supported $^{210}Pb$ (i.e., $^{226}Ra$ activity) from the total $^{210}Pb$ activity. The sediment accretion rate for the previous 120 years was estimated by two methods derived from $^{210}Pb$ dating, the Constant Initial Concentration (CIC) model assuming that this rate has not varied during the encompassed time span (Appleby and Oldfield 1992), and the Constant Rate of Supply (CRS) model based on a constant influx of unsupported, atmospheric $^{210}Pb$ that allows a variable sediment rate (Ivanovich and Harmon 1992). Organic carbon accumulation rates were estimated from sediment accretion rates (mm $yr^{-1}$), dry bulk density (g $cm^{-3}$) and OC content.

The land/use cover analysis was based on documented historical information before 1975 and satellite images (Landsat/SRTM, Table 1) from 1975, 1985, 1995 and 2008 available from the United States Geological Survey (USGS). No significant deforestation occurred in the catchment area of the Jupindá Lake until early 1940's (Amorim 2000, Cruz et al. 2011). Subsequent land/use changes were determined using satellite images (Gordon 1980, Munyati 2000). All satellite images were from low-water seasons to remove the influence of the flood pulse on the exposed area over years. The resolution of the images was 30 m, except that from the 1970's which was resampled from 90 to 30 m (Table 1). This approach allowed an assessment of changes in land cover which could then be compared to results from carbon accumulation. Results of the spatial assessment were separated into two time periods; 1942-1975, or the timeframe between the onset of land clearing and the first satellite image, and 1975-2008 which provides a more detailed assessment of temporal changes to the study area. The time period 1942-1975 was

Biogeosciences Discuss., doi:10.5194/bg-2017-151, 2017
Manuscript under review for journal Biogeosciences
Discussion started: 17 May 2017


characterized by a rapid removal (peak until the 1960's) of vegetation established at the margins of inland waters; especially *Aniba rosaeodora* (Pau-rosa) for extraction of oils, and *Mezilaurus itauba* and *Cedrela fissilis* (Louro-itaúba and Cedro, respectively) as hardwoods, and the opening of clearings for crops of textile fibers and subsistence products. Further, intensification of deforestation towards the interior of the forest and following the urban growth of Santarém is reported from the 1970's, along with depleting vegetal resources near to the margins of lakes and running waters in this region was noted (Amorim 2000, Cruz et al. 2011).

In order to address the spatial dependence of recent OC burial in Jupindá Lake for deforestation, we analyzed the land/cover use in four buffer areas around this lake and contributing rivers or streams. The first buffer of 100 m represented the riparian forest protected area by the Brazilian laws for fluvial channels with a width of 50 to 200 m. Other buffers were progressively higher, with a width of 500, 1000 and 6000 m from the riverbank and lake margins (Figure 2). In addition, we considered only stretches of rivers and streams 65-km long from Jupindá Lake to analyze its catchment area of more direct influence. This criteria also allowed to avoid the interference of the artificial flooding on the margins of the Curuá-Una hydroelectric dam, which was built in 1977 (Fearnside 2005).

## 3. Results

Analyses of $^{239+240}Pu$ were not detectable from the bottom of the sediment core until the 22-26 cm interval (Figure 43). This radioisotope was detected in the 18-22 cm

Biogeosciences Discuss., doi:10.5194/bg-2017-151, 2017
Manuscript under review for journal Biogeosciences
Discussion started: 17 May 2017


interval (0.029 ± 0.002 Bq/kg $^{239+240}$Pu) with the highest concentrations (0.047 ± 0.004 Bq/kg $^{239+240}$Pu) at the 16 cm depth. The $^{239+240}$Pu activities appears to spike at the 14 to 18 cm interval, which indicates the 1963 stratospheric fallout peak. It may be said with certainty that the material below 22 cm was deposited pre-bomb (that is, prior to the early 1950's). This affixes an upper limit on the average sedimentation rate of near to 3.8 mm year$^{-1}$. The Pu atom ratio data indicate that the Pu is originating from stratospheric fallout (plutonium isotopic ratios ($^{240/239}$Pu) of ~0.18). These results are consistent with the $^{240}$Pu/$^{239}$Pu of 0.180 ± 0.014 discussed by Kelley et al. (1999).

The $^{210}$Pb and $^{226}$Ra profiles reveal a complex depositional environment with sedimentation variations in the upper intervals with disturbances, such as bio-turbation and resuspension in the upper ~ 20 cm of the sediment column (Figure 4). A decrease in $^{210}Pb_{ex}$ activity was found below the 20 cm depth interval. The $^{210}Pb_{ex}$ data distribution are as follows: $y = -0.0749x + 7.5$) ($R^2 = 0.73$; n=19; $p < 0.01$) from the 20 to the 60 cm interval, below the apparent mixed zone. Both estimates of sediment accretion rate during the 120 years from CIC and CRS models were similar, reaching 4.1 and 4.3 mm yr$^{-1}$ respectively, which were slightly higher than the ~ 60 year $^{239+240}$Pu dates (3.8 mm yr$^{-1}$).

The dry bulk density (DBD), total organic carbon (OC%), total nitrogen (TN%) content and the carbon and nitrogen (C/N) molar ratios along with the $\delta^{13}$C and $\delta^{15}$N values showed important increases towards the center of the sediment core Table 2. The relationship between $\delta^{13}$C and $\delta^{15}$N indicated different origins of OC in the sediment core (Figure 5) contributing to the significant relationship between recent OC burial and the $\delta^{13}$C (Figure 6).

The OC burial rates show an increasing trend from ~ 1930 to 1960 with a peak during the 1940's and 50's (grey area in Figure 7). The carbon burial rates increased, from 150 g $m^{-2}$ $year^{-1}$ in the time period 1890 - 1940 to ~ 300 g $m^{-2}$ $year^{-1}$ between 1940 and 1950. Carbon accumulation then decreased to approximately 200 g $m^{-2}$ $year^{-1}$ from 1960 to 1980, after which a gradual decline in carbon burial was still measured. In relation to land use/cover in the surroundings of fluvial channels and the Jupindá lake over time, only the smallest buffer (100 m) showed more intense relative changes during the previous period 1942-1975, when the increase in deforested area was around 75 % higher than in the subsequent time period 1975-2008 (Figure 8).

## 4. Discussion

Overall, similar estimates of sediment accretion using different methodologies (i.e. 60 and 120 year trends from the $^{239+240}Pu$ and $^{210}Pb_{(ex)}$ models, respectively) revealed an insight into changes in the sediment accumulation assessed here. This indicates that even though the origin of the organic material was modified, the sediment accumulation has varied little as indicated by the 60- or 120-year sediment accumulation rates. To present the historical profiles of the carbon burial rates, an average is taken between these two methods (4 mm $year^{-1}$), multiplied by the DBD and carbon content for each interval of the entire sediment core.

The high peak in carbon accumulation observed around 1950 appears to be associated with a shift in the source of organic material, inferred by changes in carbon and nitrogen contents and the isotopic fractioning toward the middle (from 40 to 20 cm depth interval) of the sediment column. This peak for different organic and inorganic variables in intermediate depths revealed changes not only in the amount but also in the

Biogeosciences Discuss., doi:10.5194/bg-2017-151, 2017
Manuscript under review for journal Biogeosciences
Discussion started: 17 May 2017


type of material being deposited over time. Previous studies have reported two common origins for OC in the Amazon forest. Higher $\delta^{15}N$ and more negative $\delta^{13}C$ values could indicate the presence of Santarém soil organic matter (such as that adjacent to the Jupindá Lake), while lower $\delta^{15}N$ and more variable $\delta^{13}C$ values indicate particulate organic carbon (POC) from the terrestrial vegetation in the catchment (Ometto et al. 2006, Zocatelli et al. 2013). Here, a corresponding increase in OC%, TN% and OC burial rates measured, with a peak near ~1950, suggesting higher inputs of organic matter into lake. The higher $\delta^{13}C$ signature, coupled with a lower $\delta^{15}N$ indicates a greater influence from the terrestrial Amazonian POC during the same period around 1950 (Ometto et al., 2006).

When looking for a cause for this change in the source of organic material, we look to the analysis of land use change. Land clearing associated with early occupation from the 1940s in the catchment area of the Jupindá Lake reveals a potential cause of the increased carbon burial observed in this lake. Changes in land use and cover may significantly affect recent OC burial in mid-high-latitude lakes (Anderson et al. 2013, Dietz et al. 2015). Our results suggest that land clearing during the 1940's and 50's might be related to increased organic matter deposition in the region's floodplain lakes. During this period, intense wood extraction and expansion of agricultural settlements occurred (Amorim 2000, Cruz et al. 2011). One important consequence of deforestation in the watershed is the silting up of lakes (Enea et al. 2012 ), including those at humid low-latitude areas (Cohen et al. 2005, Bakoariniaina et al. 2006). The riparian forest systems are generally effective in reducing the sediment transport by surface runoff, with the removal of this vegetation increasing the erosion processes especially in the Amazon basin due to intense rainfall (Neill et al. 2013a).

Biogeosciences Discuss., doi:10.5194/bg-2017-151, 2017
Manuscript under review for journal Biogeosciences
Discussion started: 17 May 2017


We also found a spatial dependence of the carbon accumulation in the Lake Jupindá, as the much lower OC burial was coupled to higher deforestation rates in those larger buffers around its margins and main fluvial channels (500, 1000 and 6000 m) in the period after 1975 (1975-2008) than that before (1942-1975). This confirms previous evidences that the recent deforestation process in the region was started in areas around running and lake waters (Amorim 2000, Cruz et al. 2011), and not in the interior of the forest. The enhanced OC burial in lacustrine sediments before 1975 was related to higher deforestation rates only in the riparian vegetation zone (100-m buffers), suggesting a higher influence of deforestation with decreasing distance to water courses. Therefore, the soil carbon enrichment to the aquatic sediments during the peaks of riparian deforestation may cause intense but temporary carbon burial events in the Amazon floodplain, representing a significant part of the total loss of terrestrial organic matter. In contrast, the continued removal of vegetation from the interior of the forest might be not directly related to increases of OC burial, even temporarily, in depositional aquatic ecosystems.

## 5. Conclusion

The $^{239+240}$Pu and $^{210}$Pb dating methods were combined with a spatial analysis of vegetation clearing to firstly calculate carbon accumulation rates, and then to interpret changes in sediment characteristics during the previous century. The Pu dating method closely approximates measurements from the $^{210}$Pb chronologies and hence offers mechanism to determine sedimentation rates and carbon accumulation in Amazon sediments. An increase in OC burial, 150 to ~ 300 OC g m$^{-2}$ year$^{-1}$, coincides with changes in the $\delta^{13}C$ and $\delta^{15}N$ signatures, likely influenced by the heavy deforestation in riparian systems of this region during the 1940s and 50's. It is therefore suggested that the net increase in carbon burial towards the center of the sediment core, which represents the highest carbon burial rates during the 1950s, is a result of a change in source of organic matter deposition. The differing carbon burial rates along the sediment core reveals the potential complexity of carbon burial rates in the Amazon floodplain lakes, directly related to the development within the Basin. This work demonstrates a new understanding on spatial dependence of carbon burial capacity of the Amazon floodplain lakes with respect to advances in deforestation in the basin.

**Acknowledgements**

LMS is supported by an APA and IPRS scholarships. HM received a research grant from the Brazilian Research Council (CNPq – "Programa Universal") and the Research Support Foundation of the State of Rio de Janeiro (FAPERJ – "Programa Jovem Cientista do Nosso Estado").

## CAPTIONS TO FIGURES

**Figure 1.** Floodplain Lake where the sediment core was collect, near the Amazon River and the city of Santarém, Brazil. This floodplain lake has a diameter of approximately 3 km.

Biogeosciences Discuss., doi:10.5194/bg-2017-151, 2017
Manuscript under review for journal Biogeosciences
Discussion started: 17 May 2017


**Figure 2.** Different buffer sizes (100m, 500m, 1km and 6km) along the stretch of the Curuá-Una river from Jupindá Lake (red) to the hydroelectric dam upstream (yellow).

**Figure 3.** $^{239+240}$Pu profile, indicating ~ 1950 when these radionuclides were first introduced into the atmosphere.

**Figure 4.** Excess $^{210}$Pb and $^{226}$Ra profile against depth.

**Figure 5.** $\delta^{13}$C vs $\delta^{15}$N. The Amazon River POM and Santarem soil organic matter values, adjacent to the study area, are taken from Zocatelli et al (2013).

**Figure 6.** Carbon burial as a function of $\delta^{13}$C.

**Figure 7**. $\delta^{13}$C, $\delta^{15}$N and carbon burial rate values in relation to age (year).

**Figure 8.** Percentage of modified areas in relation to the different buffers.

**CAPTION TO TABLES**

**Table 1**. Satellite acquisition data from United States Geological Survey (USGS) and the Curuá-Una River quota from Brazilian Water Agency (ANA).

**Table 2.** Depth profiles of dry bulk density (DBD), total organic carbon (OC%), total nitrogen (TN%) carbon and nitrogen (C/N) molar ratios, $\delta^{13}$C and $\delta^{15}$N.

**Table 1.**

| ***Month/Year*** | ***Landsat Data*** | ***Curuá-Una River Quote*** |
|---|---|---|
| Aug/1975 | 2 | 5.3 |
| Oct/1985 | 5 | 3.7 |
| June/1995 | 5 | 6 |
| June/2008 | 5 | *No data* |

**Table 2.**

| Depth (cm) | DBD (g cm$^{-3}$) | $\delta^{15}N$ | $\delta^{13}C$ | C (%) | N (%) | C/N |
|---|---|---|---|---|---|---|
| 0-2 | 1.0 | 8.9 | -29.2 | 3.8 | 0.3 | 17.2 |
| 2-4 | 0.9 | 11.7 | -29.0 | 3.8 | 0.3 | 18.7 |
| 4-6 | 1.0 | 10.4 | -28.8 | 4.0 | 0.3 | 19.2 |
| 6-8 | 1.1 | 9.3 | -28.7 | 4.3 | 0.3 | 20.2 |
| 8-10 | 1.0 | 9.4 | -28.7 | 4.1 | 0.3 | 19.8 |
| 10-12 | 1.1 | 7.9 | -28.6 | 4.6 | 0.3 | 21.2 |
| 12-14 | 1.1 | 8.2 | -28.7 | 4.3 | 0.3 | 19.9 |
| 14-16 | 1.1 | 7.8 | -28.6 | 4.3 | 0.3 | 20.9 |
| 16-18 | 1.0 | 8.7 | -28.5 | 4.4 | 0.3 | 21.2 |
| 18-20 | 1.1 | 7.5 | -28.4 | 4.4 | 0.3 | 19.8 |
| 20-22 | 1.0 | 6.5 | -28.2 | 5.4 | 0.3 | 21.2 |
| 22-24 | 1.0 | 6.0 | -27.8 | 5.3 | 0.3 | 21.5 |
| 24-26 | 1.0 | 5.2 | -27.4 | 7.3 | 0.4 | 25.4 |
| 26-28 | 1.1 | 6.1 | -27.6 | 6.0 | 0.3 | 23.8 |
| 28-30 | 1.0 | 5.0 | -27.3 | 6.0 | 0.4 | 22.7 |
| 30-32 | 1.0 | 5.4 | -28.0 | 6.1 | 0.3 | 27.0 |
| 32-34 | 1.3 | 6.6 | -28.5 | 4.4 | 0.2 | 27.5 |
| 34-36 | 1.6 | 8.9 | -29.0 | 2.2 | 0.1 | 23.1 |
| 36-38 | 1.4 | 11.4 | -29.4 | 2.9 | 0.1 | 30.4 |
| 38-40 | 1.4 | 10.4 | -29.5 | 3.3 | 0.1 | 30.5 |
| 40-42 | 1.5 | 11.4 | -29.3 | 2.4 | 0.1 | 23.8 |
| 42-44 | 1.6 | 12.2 | -29.4 | 1.3 | 0.1 | 15.6 |
| 44-46 | 1.8 | 8.2 | -29.6 | 1.2 | 0.1 | 14.3 |
| 46-48 | 1.5 | 8.8 | -29.8 | 2.2 | 0.1 | 21.6 |
| 48-50 | 0.9 | 10.4 | -29.7 | 2.9 | 0.2 | 25.6 |
| 50-52 | 0.9 | 10.2 | -29.7 | 2.6 | 0.1 | 27.2 |
| 52-54 | 0.9 | 7.1 | -29.7 | 3.9 | 0.2 | 28.6 |
| 54-56 | 0.9 | 9.2 | -29.9 | 3.6 | 0.2 | 27.8 |
| 56-58 | 0.9 | 6.6 | -30.1 | 4.3 | 0.2 | 30.1 |
| 58-60 | 0.9 | 5.0 | -30.1 | 3.5 | 0.2 | 23.1 |
| **Average** | **1.11** | **8.34** | **-28.9** | **4.0** | **0.2** | **23.0** |
| **Stand Dev** | **0.24** | **2.1** | **0.8** | **1.9** | **0.1** | **4.2** |

Biogeosciences Discuss., doi:10.5194/bg-2017-151, 2017
Manuscript under review for journal Biogeosciences
Discussion started: 17 May 2017


**References**

Aalto, R., L. Maurice-Bourgoin, T. Dunne, D. R. Montgomery, C. A. Nittrouer, and J. L. Guyot. 2003. Episodic sediment accumulation on Amazonian flood plains influenced by El Niño/Southern Oscillation. Nature **425**:493-497.

Abril, G., J. M. Martinez, L. F. Artigas, P. Moreira-Turcq, M. F. Benedetti, L. Vidal, T. Meziane, J. H. Kim, M. C. Bernardes, N. Savoye, J. Deborde, E. L. Souza, P. Albéric, M. F. Landim De Souza, and F. Roland. 2014. Amazon River carbon dioxide outgassing fuelled by wetlands. Nature **505**:395-398.

Amorim, A. T. d. S. 2000. Santarém: uma síntese histórica, Canoas, Ulbra, Santarem, Brazil

Anderson, N. J., R. D. Dietz, and D. R. Engstrom. 2013. Land-use change, not climate, controls organic carbon burial in lakes. Proceedings. Biological sciences / The Royal Society **280**:20131278.

Appleby, P. G., and F. Oldfield. 1992. Application of lead-210 to sedimentation studies. Pages 731-783 *in* M. Ivanovich and S. Harmon, editors. Uranium Series Disequilibrium: Application to Earth, Marine and Environmental Science. Oxford Science Publications.

Bakoariniaina, L. N., T. Kusky, and T. Raharimahefa. 2006. Disappearing Lake Alaotra: Monitoring catastrophic erosion, waterway silting, and land degradation hazards in Madagascar using Landsat imagery. Journal of African Earth Sciences **44**:241-252.

Cohen, A. S., M. R. Palacios-Fest, J. McGill, P. W. Swarzenski, D. Verschuren, R. Sinyinza, T. Songori, B. Kakagozo, M. Syampila, C. M. O'Reilly, and S. R. Alin. 2005. Paleolimnological investigations of anthropogenic environmental change in

Biogeosciences Discuss., doi:10.5194/bg-2017-151, 2017
Manuscript under review for journal Biogeosciences
Discussion started: 17 May 2017


Lake Tanganyika: I. An introduction to the project. Journal of Paleolimnology **34**:1-18.

Cruz, H., P. Sablayrolles, M. Kanashiro, and M. S. Amaral, P. 2011. Relação empresa/ comunidade no manejo florestal comunitário e familiar: Uma contribuição do Projeto Floresta em pé.

Diaz, R. J., and R. Rosenberg. 2008. Spreading dead zones and consequences for marine ecosystems. Science **321**:926-929.

Dietz, R. D., D. R. Engstrom, and N. J. Anderson. 2015. Patterns and drivers of change in organic carbon burial across a diverse landscape: Insights from 116 Minnesota lakes. Global Biogeochemical Cycles **29**:708-727.

Dong, X., N. J. Anderson, X. Yang, X. chen, and J. Shen. 2012. Carbon burial by shallow lakes on the Yangtze floodplain and its relevance to regional carbon sequestration. Global Change Biology **18**:2205-2217.

Downing, J. P., M. Meybeck, J. C. Orr, R. R. Twilley, and H. W. Scharpenseel. 1993. Land and water interface zones. Water, Air, & Soil Pollution **70**:123-137.

Enea, A., G. Romanescu, and C. Stoleriu. 2012 Quantitative considerations concerning the source-areas for the silting of the red lake (Romania) lacustrine basin. Romania.

Fearnside, P. M. 2005. Do hydroelectric dams mitigate global warming? The case of Brazil's Curuá-Una Dam. Mitigation and Adaptation Strategies for Global Change **10**:675-691.

Gordon, S. I. 1980. Utilizing LANDSAT imagery to monitor land-use change: A case study in ohio. Remote Sensing of Environment **9**:189-196.

Biogeosciences Discuss., doi:10.5194/bg-2017-151, 2017
Manuscript under review for journal Biogeosciences
Discussion started: 17 May 2017


Goulding, M. 1993. Flooded forests of the Amazon. Scientific American **268**:114-120+115.

Hoffmann, T., M. Schlummer, B. Notebaert, G. Verstraeten, and O. Korup. 2013. Carbon burial in soil sediments from Holocene agricultural erosion, Central Europe. Global Biogeochemical Cycles **27**:828-835.

INPE. 2016. Program for the Estimation of Amazon Deforestation. Accessed 20 November 2016, http://www.obt.inpe.br/prodes/prodes_1988_2015n.htm.

Ivanovich, M., and S. Harmon. 1992. Uranium Series Disequilibrium - Applications to Earth, Marine and Environmental Sciences. second edition edition. Oxford Science Publications.

Junk, W. J. 2013. Current state of knowledge regarding South America wetlands and their future under global climate change. Aquatic Sciences **75**:113-131.

Ketterer, M. E., K. M. Hafer, V. J. Jones, and P. G. Appleby. 2004. Rapid dating of recent sediments in Loch Ness: Inductively coupled plasma mass spectrometric measurements of global fallout plutonium. Science of the Total Environment **322**:221-229.

LigockI, L. P. 2003. Comportamento geotécnico da barragem de Curuá-Una, Pará. Rio de Janeiro.

Lucas, C. M., J. Schöngart, P. Sheikh, F. Wittmann, M. T. F. Piedade, and D. G. McGrath. 2014. Effects of land-use and hydroperiod on aboveground biomass and productivity of secondary Amazonian floodplain forests. Forest Ecology and Management **319**:116-127.

Biogeosciences Discuss., doi:10.5194/bg-2017-151, 2017
Manuscript under review for journal Biogeosciences
Discussion started: 17 May 2017


Marotta, H., L. Bento, F. A. De Esteves, and A. Enrich-Prast. 2009. Whole ecosystem evidence of eutrophication enhancement by wetland dredging in a shallow Tropical Lake. Estuaries and Coasts **32**:654-660.

Marotta, H., C. M. Duarte, F. Meirelles-Pereira, L. Bento, F. A. Esteves, and A. Enrich-Prast. 2010. Long-term CO2 variability in two shallow tropical lakes experiencing episodic eutrophication and acidification events. Ecosystems **13**:382-392.

Marotta, H., L. Pinho, C. Gudasz, D. Bastviken, L. J. Tranvik, and A. Enrich-Prast. 2014. Greenhouse gas production in low-latitude lake sediments responds strongly to warming. Nature Climate Change **4**:467-470.

Melack, J. M., L. L. Hess, M. Gastil, B. R. Forsberg, S. K. Hamilton, I. B. T. Lima, and E. M. L. M. Novo. 2004. Regionalization of methane emissions in the Amazon Basin with microwave remote sensing. Global Change Biology **10**:530-544.

Moreira-Turcq, P., J. M. Jouanneau, B. Turcq, P. Seyler, O. Weber, and J. L. Guyot. 2004. Carbon sedimentation at Lago Grande de Curuai, a floodplain lake in the low Amazon region: Insights into sedimentation rates. Palaeogeography, Palaeoclimatology, Palaeoecology **214**:27-40.

Munyati, C. 2000. Wetland change detection on the Kafue Flats, Zambia, by classification of a multitemporal remote sensing image dataset. International Journal of Remote Sensing **21**:1787-1806.

Neill, C., M. T. Coe, S. H. Riskin, A. V. Krusche, H. Elsenbeer, M. N. Macedo, R. McHorney, P. Lefebvre, E. A. Davidson, R. Scheffler, A. M. e Silva Figueira, S. Porder, and L. A. Deegan. 2013a. Watershed responses to Amazon soya bean cropland expansion and intensification. Philosophical Transactions of the Royal Society B: Biological Sciences **368**.

Neill, C., M. T. Coe, S. H. Riskin, A. V. Krusche, H. Elsenbeer, M. N. Macedo, R. McHorney, P. Lefebvre, E. A. Davidson, R. Scheffler, A. M. Figueira, S. Porder, and L. A. Deegan. 2013b. Watershed responses to Amazon soya bean cropland expansion and intensification. Philosophical transactions of the Royal Society of London. Series B, Biological sciences **368**:20120425.

Neue, H. U., J. L. Gaunt, Z. P. Wang, P. Becker-Heidmann, and C. Quijano. 1997. Carbon in tropical wetlands. Geoderma **79**:163-185.

Ometto, J. P. H. B., J. R. Ehleringer, T. F. Domingues, J. A. Berry, F. Y. Ishida, E. Mazzi, N. Higuchi, L. B. Flanagan, G. B. Nardoto, and L. A. Martinelli. 2006. The stable carbon and nitrogen isotopic composition of vegetation in tropical forests of the Amazon Basin, Brazil. Biogeochemistry **79**:251-274.

Peixoto, R. B., H. Marotta, D. Bastviken, and A. Enrich-Prast. 2016. Floating Aquatic Macrophytes Can Substantially Offset Open Water CO<inf>2</inf> Emissions from Tropical Floodplain Lake Ecosystems. Ecosystems **19**:724-736.

Sanders, C. J., B. D. Eyre, I. R. Santos, W. MacHado, W. Luiz-Silva, J. M. Smoak, J. L. Breithaupt, M. E. Ketterer, L. Sanders, H. Marotta, and E. Silva-Filho. 2014. Elevated rates of organic carbon, nitrogen, and phosphorus accumulation in a highly impacted mangrove wetland. Geophysical Research Letters **41**:2475-2480.

Sanders, L. M., K. H. Taffs, D. J. Stokes, C. J. Sanders, J. M. Smoak, A. Enrich-Prast, P. Macklin, I. R. Santos, and H. Marotta. 2017. Carbon accumulation in Amazonian floodplain lakes: A significant component of Amazon budgets? Limnology & Oceanography Letters:29-35.

Skole, D., and C. Tucker. 1993. Tropical deforestation and habitat fragmentation in the amazon: Satellite data from 1978 to 1988. Science **260**:1905-1910.

Smith, L. K., J. M. Melack, and D. E. Hammond. 2002. Carbon, nitrogen, and phosphorus content and 210Pb-derived burial rates in sediments of an Amazon floodplain lake. Amazoniana **17**:413-436.

Stanley, E. H., S. M. Powers, N. R. Lottig, I. Buffam, and J. T. Crawford. 2012. Contemporary changes in dissolved organic carbon (DOC) in human-dominated rivers: Is there a role for DOC management? Freshwater Biology **57**:26-42.

Zocatelli, R., P. Moreira-Turcq, M. Bernardes, B. Turcq, R. C. Cordeiro, S. Gogo, J. R. Disnar, and M. Boussafir. 2013. Sedimentary evidence of soil organic matter input to the curuai amazonian floodplain. Organic Geochemistry **63**:40-47.

**Figure 1.**

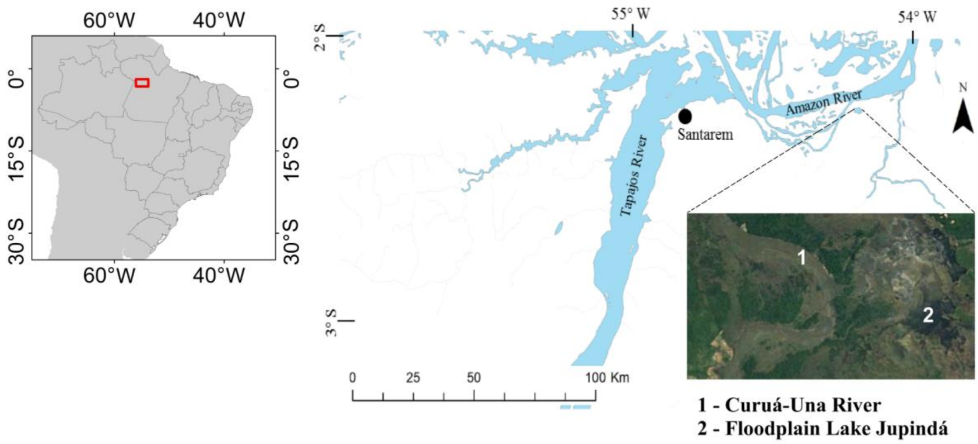
60°W
40°W
0°
15°S
30°S
55° W
54° W
2° S
3° S
Amazon River
Santarem
Tapajos River
N
1
2
0
25
50
100 Km
1 - Curuá-Una River
2 - Floodplain Lake Jupindá

Biogeosciences Discuss., doi:10.5194/bg-2017-151, 2017
Manuscript under review for journal Biogeosciences
Discussion started: 17 May 2017


**Figure 2.**

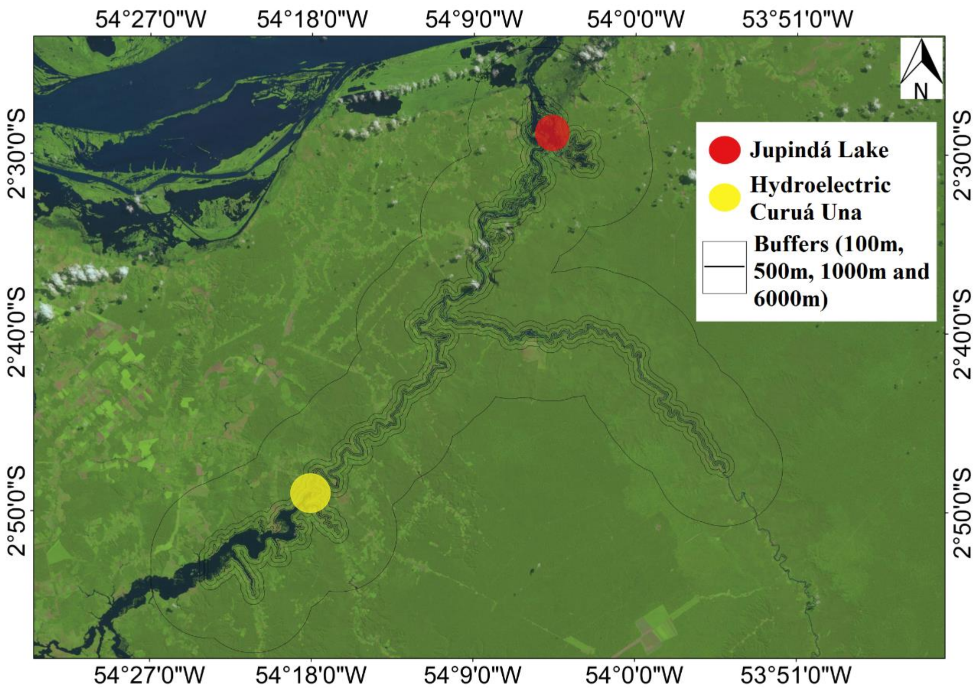

**Figure 3.**

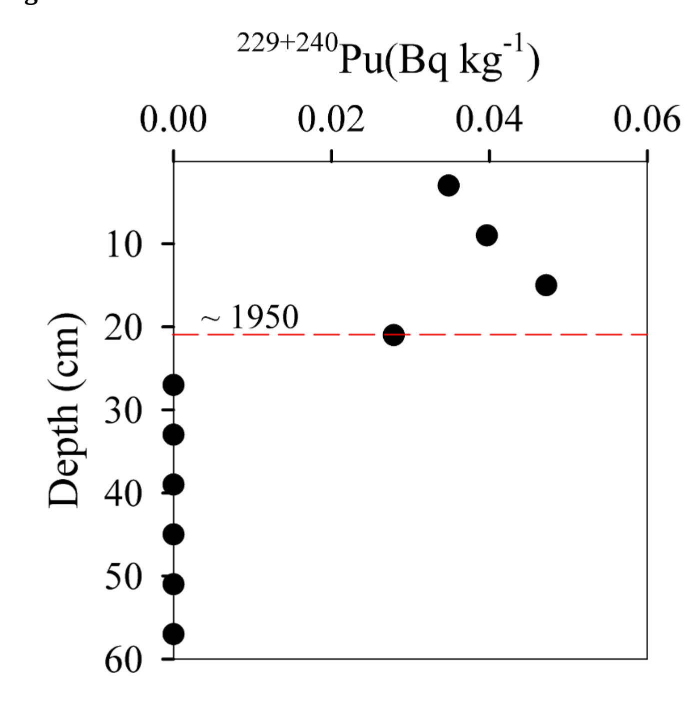

**Figure 4.**

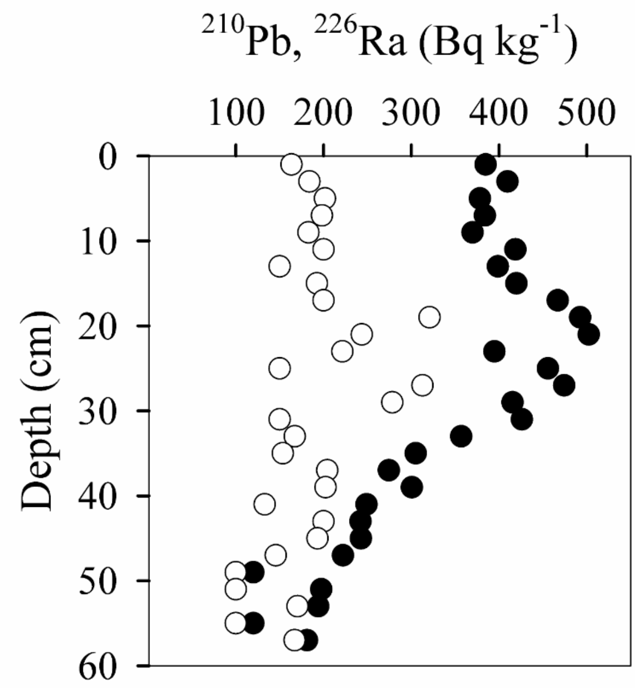
210Pb, 226Ra (Bq kg-1)
100 200 300 400 500
Depth (cm)
0
10
20
30
40
50
60

Biogeosciences Discuss., doi:10.5194/bg-2017-151, 2017
Manuscript under review for journal Biogeosciences
Discussion started: 17 May 2017


**Figure 5.**

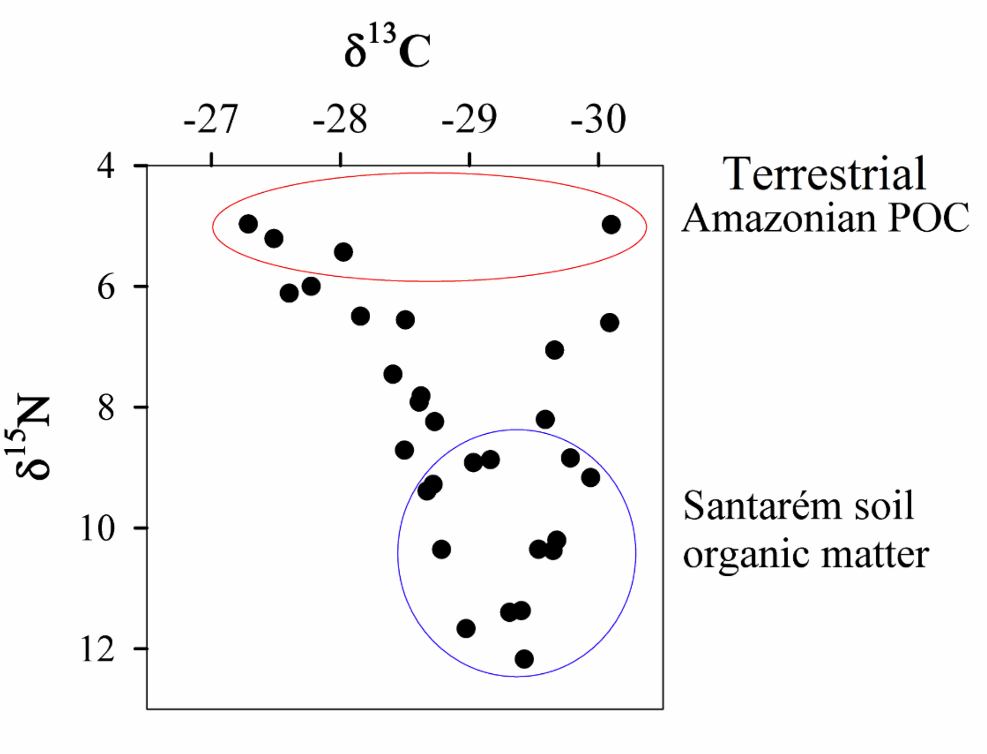

Biogeosciences Discuss., doi:10.5194/bg-2017-151, 2017
Manuscript under review for journal Biogeosciences
Discussion started: 17 May 2017


**Figure 6.**

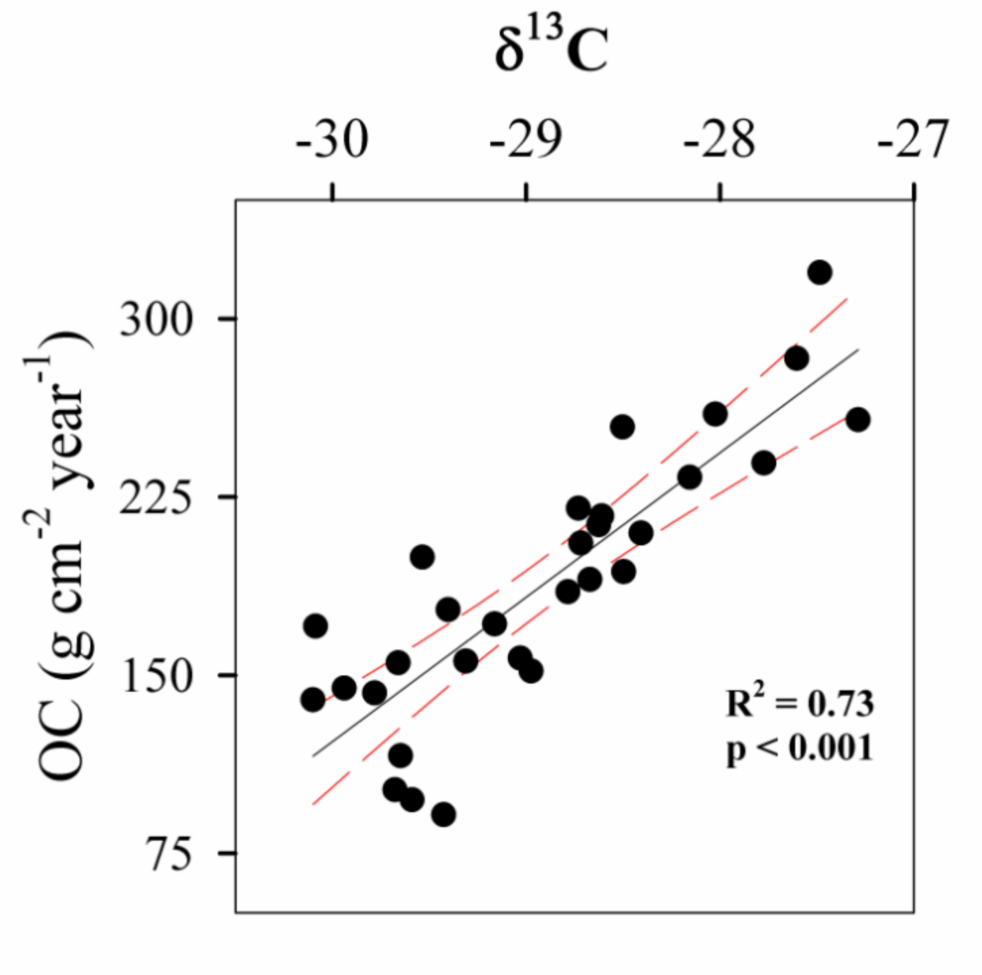

**Figure 7.**

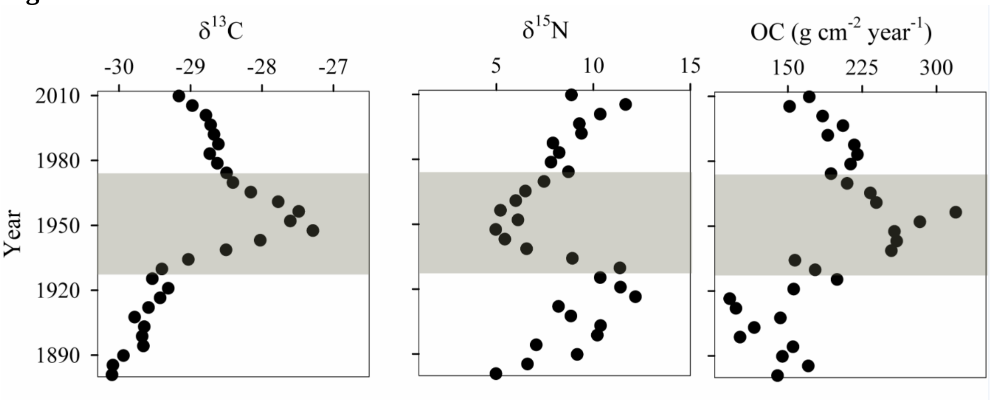
δ13C
-30
-29
-28
-27
δ15N
5
10
15
OC (g cm-2 year-1)
150
225
300
Year
2010
1980
1950
1920
1890

**Figure 8.**

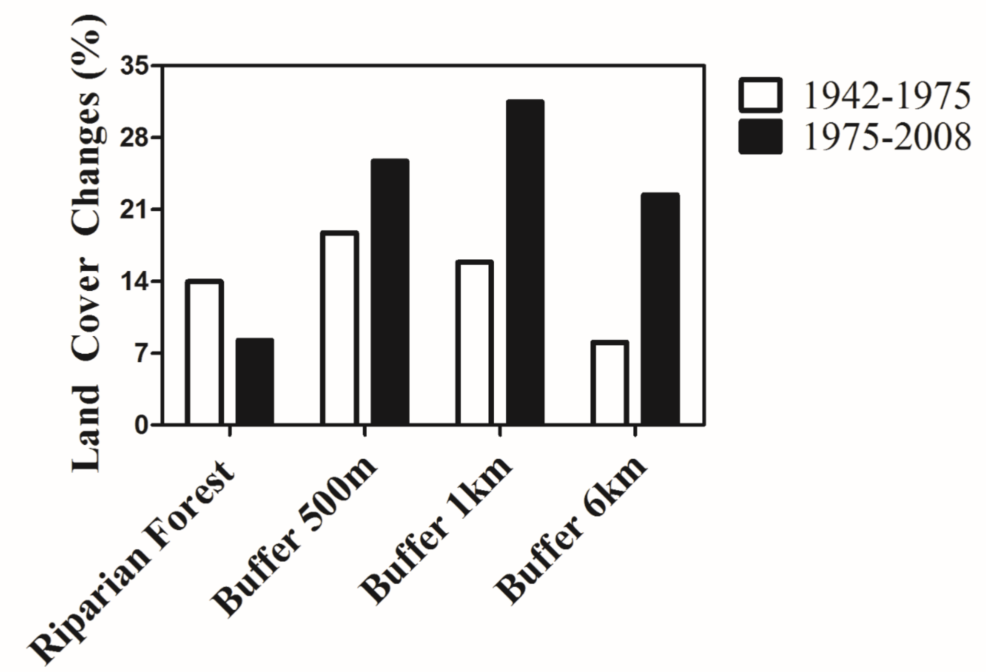
Land Cover Changes (%)
35
28
21
14
7
0
1942-1975
1975-2008
Riparian Forest
Buffer 500m
Buffer 1km
Buffer 6km